

Temperature dependence of the 2D-3D transition in the growth of PTCDA on Ag(111): A real-time X-ray and kinetic Monte Carlo study

B. KRAUSE^{1(*)}, F. SCHREIBER^{1,2(**)}, H. DOSCH^{1,2},
A. PIMPINELLI³ and O. H. SEECK⁴

¹ *Max-Planck-Institut für Metallforschung - Heisenbergstr. 3
D-70569 Stuttgart, Germany*

² *Institut für Theoretische und Angewandte Physik, Universität Stuttgart
Pfaffenwaldring 57, D-70550 Stuttgart, Germany*

³ *LASMEA, Université Blaise Pascal - Clermont 2, Les Cézeaux
63177 Aubière Cedex, France*

⁴ *IFF, Forschungszentrum Jülich GmbH - D-52425 Jülich, Germany*

(received 7 July 2003; accepted in final form 21 November 2003)

PACS. 68.55.Ac – Nucleation and growth: microscopic aspects.

PACS. 81.10.Aj – Theory and models of crystal growth; physics of crystal growth, crystal morphology and orientation.

PACS. 61.66.Hq – Organic compounds.

Abstract. – We present a real-time X-ray scattering study of the growth modes in organic molecular-beam epitaxy. We have studied the model system 3,4,9,10-perylene-tetracarboxylic dianhydride (PTCDA) on Ag(111) and find a temperature-dependent transition from layer-by-layer growth to islanding. The transition smears out for low substrate temperatures, T , implying that the degree of the layer-by-layer growth of the wetting layer decreases with decreasing T . This behavior has been analyzed quantitatively and reproduced by kinetic Monte Carlo simulations. The implications and consequences of our findings for the understanding of the organic molecular-beam epitaxy are discussed.

Organic semiconducting compounds are attracting much attention in basic research and technology due to their interesting electronic and optical properties. It has become evident that the exploitation of the full potential of these materials requires the understanding and control of the structures on a molecular level. This presents a serious challenge, since there are obviously significant differences compared to inorganic semiconductors in terms of the interactions involved and also the shape anisotropy inherent in most of these molecules. While the thermodynamically stable structure has been characterized for certain systems,

(*) New address: European Synchrotron Radiation Facility, ESRF - B.P. 220, F-38043 Grenoble Cedex, France.

(**) New address: Physical and Theoretical Chemistry Laboratory, Oxford University - South Parks Road, Oxford, OX1 3QZ, UK.

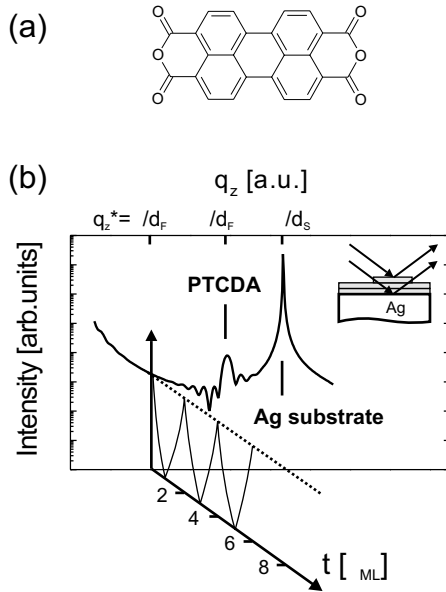


Fig. 1

Fig. 1 – (a) Schematic of the molecule 3,4,9,10-perylenetetracarboxylic dianhydride (PTCDA). (b) Simulation of the specular rod of a thin PTCDA film on Ag(111). At the anti-Bragg point of the PTCDA film ($q_z^* = \pi/d_F$), the scattering of subsequent layers interferes destructively (see inset). For layer-by-layer growth, the intensity at the anti-Bragg point oscillates as a function of the deposition time.

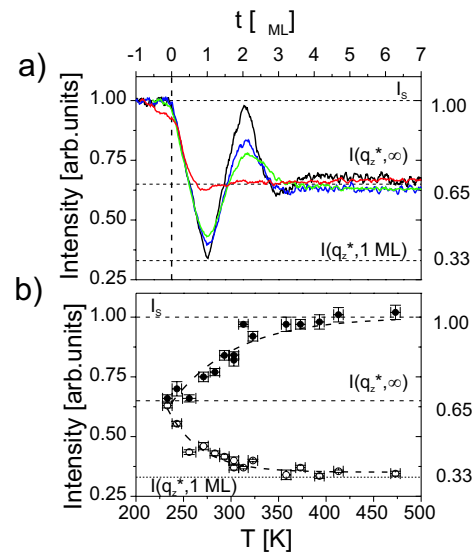


Fig. 2

Fig. 2 – (a) Time-dependence of the scattered X-ray intensity during growth at various temperatures at low growth rate ($0.8\text{--}2 \text{ \AA}/\text{min}$) for $T = 233 \text{ K}$ (red), $T = 283 \text{ K}$ (green), $T = 303 \text{ K}$ (blue), and $T = 358 \text{ K}$ (black). (b) Temperature dependence of the deviation from layer-by-layer growth expressed in terms of the intensity of the minimum (open symbols) and of the maximum (filled symbols) scattered intensity at 1 ML and 2 ML, respectively. The dashed lines indicate the intensity scattered by the substrate, $I_S = 1$, the intensity scattered by 1 ML PTCDA, $I(q_z^*, \tau_{ML}) = 0.33$, and the asymptotic scattering intensity for large t , $I(q_z^*, \infty) = 0.65$.

the morphology depends strongly on the growth kinetics, which is much less understood. Moreover, it is not obvious how the general description of growth modes compares to that of inorganic materials, since the internal degrees of freedom (including molecular orientation) may give rise to new phenomena.

One method particularly suitable for the controlled growth of organic thin films is organic molecular-beam epitaxy (OMBE) [1]. In many cases a transition from layer-by-layer growth to islanding, *i.e.* Stranski-Krastanov (SK) growth, has been observed [2–4] which is also common for inorganic heteroepitaxy [5]. The dynamics and the temperature dependence of this 2D-3D transition are fundamental aspects of heteroepitaxial growth which are, however, only poorly understood [6].

In this letter, we present an X-ray diffraction study of Stranski-Krastanov growth of 3,4,9,10-perylenetetracarboxylic dianhydride (PTCDA, fig. 1(a)) on Ag(111) as an archetypal system for OMBE. In contrast to most previous studies [7–9], we focus on the temperature dependence of the formation of the wetting layer and the kinetics of the subsequent 2D-3D

transition. We show that the growth mode of the wetting layer changes as a function of temperature. A quantitative measure of this transition is introduced which can be applied to the experiment without referring to any complex theoretical models. The experimental observations are compared with kinetic Monte Carlo simulations which simulate time-dependent processes such as growth in contrast to equilibrium states.

PTCDA is a flat molecule which exhibits a regular stacking along the crystallographic (102) direction of the bulk crystal. On Ag(111), epitaxial growth of PTCDA(102) has been observed [3, 10, 11]. At growth temperatures $T \lesssim 350$ K, relatively smooth but strained epitaxial films have been found, whereas at $T \gtrsim 350$ K, separate crystallites with bulk crystalline structure on top of a 2 ML thick wetting layer have been observed [3, 4]. The PTCDA films have an out-of-plane lattice spacing of about 3.2 \AA as derived from specular rod measurements [12]. Due to the well-defined structure of PTCDA on Ag(111), this system is very suitable for the study of fundamental growth processes.

In order to follow the growth of thin PTCDA films, the X-ray diffraction intensity from the molecular layers has been measured in real time. In kinematic theory, the specular X-ray scattering intensity is the sum of the scattering contributions from the film and the substrate,

$$I(q_z, t) = |F(q_z, t)|^2 = \left| f_F \sum_{n=1}^{\infty} e^{iq_z d_F(n-1)} \theta_n(t) + f_S \frac{1}{1 - e^{-iq_z d_S}} e^{-iq_z d_0} \right|^2. \quad (1)$$

f_F and f_S are the form factors of the film and the substrate, d_F and d_S are the corresponding lattice spacings, and $d_0 = 2.8 \text{ \AA}$ is the distance between the substrate and the first layer of the film [3]. $\theta_n(t)$ is the time-dependent fractional coverage of the n -th layer within the organic film. At the anti-Bragg point of the PTCDA film ($q_z^* = \pi/d_F$) the first term in eq. (1) equals $f_F \sum (-1)^{(n-1)} \theta_n(t)$. Therefore, the coverage difference

$$\Delta\theta(t) = \sum_m \theta_{2m+1}(t) - \sum_m \theta_{2m}(t) = \theta_{\text{odd}}(t) - \theta_{\text{even}}(t) \quad (2)$$

can be deduced from the measured intensity $I(q_z^*, t)$. Specifically, it is possible to distinguish the coverage of the first and the second layer in the initial stage of the growth. In the case of layer-by-layer growth, characteristic intensity oscillations are observed [13, 14] (see fig. 1(b)). Note that the additional interference with the substrate amplitude (second term in eq. (1)) modifies this oscillatory behavior in a characteristic way, depending on the ratio of the electron densities involved and the phase factor $\exp[-iq_z d_0]$.

While this type of X-ray experiment does not give information about the lateral material distribution, it has the great advantage that it can be performed without growth interruption. This has proven to be essential for studying the growth of PTCDA. The strong post-growth diffusion of the molecules leads to a reordering of material so that the material distribution observed after growth differs significantly from the material distribution observed during the deposition [12].

The experiments have been performed at the HASYLAB at beamline W1 in a portable UHV chamber fully equipped for *in situ* studies of organic film deposition [15]. The organic thin films have been deposited at low deposition rate ($R = 0.8\text{--}2 \text{ \AA}/\text{min}$). The substrate temperature, T , during growth has been varied between 197 K and 473 K. Within the experimental uncertainties, in this temperature range no significant change in the molecular sticking coefficient has been observed.

Figure 2(a) shows typical time-dependent intensity measurements during growth, measured at various substrate temperatures between 233 and 258 K. $t = 0$ is defined as the starting time

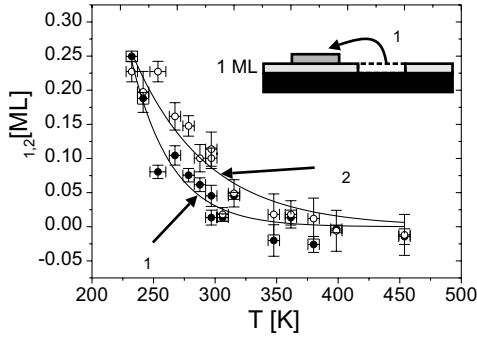


Fig. 3

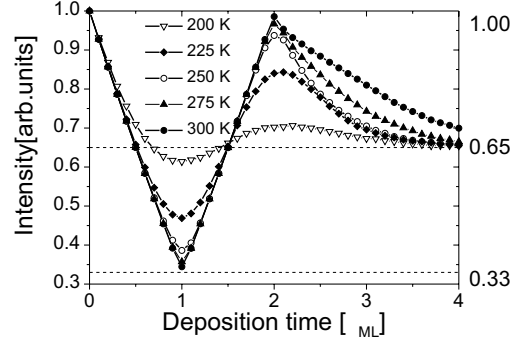


Fig. 4

Fig. 3 – Temperature dependence of the deviation from layer-by-layer growth quantified in terms of δ_1 and δ_2 . The inset explains the quantity δ_1 .

Fig. 4 – Scattered intensity calculated from the kinetic Monte Carlo simulations (see text).

of the deposition. The signal is normalized to the substrate scattering, $I_S = I(q_z^*, t < 0)$, and the time is normalized to the deposition time, τ_{ML} , of one monolayer, which corresponds to the intensity minimum. A typical growth measurement exhibits distinct intensity oscillations for $t \lesssim 3\tau_{\text{ML}}$, followed by a constant intensity during further deposition, similar to the observations for PTCDA/Au(111) [9]. The intensity oscillations correspond to layer-by-layer growth. The transition to a constant intensity indicates the breakdown of layer-by-layer growth and the onset of islanding characteristic of SK growth. As can be seen from the transition to a time-independent scattering signal (associated with an equal probability for a given molecule to be accommodated in even and odd layers), the islanding starts rapidly after completion of a 2 ML “wetting” layer.

Comparing the growth data for different temperatures (fig. 2(a)), we find that for $T \geq 358\text{ K}$ the oscillations are not visibly damped for $t < 2\tau_{\text{ML}}$. They are followed by a sharp transition to a time-independent intensity (islanding). We observe three characteristic intensity levels: The minimum intensity $I(q_z^*, \tau_{\text{ML}}) = 0.33$ corresponding to one smooth ML of PTCDA, the maximum intensity $I(q_z^*, 2\tau_{\text{ML}}) = 1$ corresponding to two smooth monolayers of PTCDA, and the temperature-independent asymptotic value $I(q_z^*, \infty) = 0.65$ (see fig. 2). For lower temperatures, the oscillations are progressively damped, and the 2D-3D transition is smeared out as the temperature is lowered. Interestingly, the asymptotic intensity is in all cases approximately 0.65, which can be shown to correspond to $\theta_{\text{odd}}(t) = \theta_{\text{even}}(t) + 0.5\text{ ML}$. This observation is consistent with a Gaussian roughness profile after the initial layer-by-layer growth. For $T < 233\text{ K}$, instead of oscillations, only a monotonic decay of the intensity is observed, approaching the asymptotic value 0.65 for long times. With increased damping (*i.e.* lower T), the position of the maximum shifts to coverages higher than 2 ML (the value expected for ideal layer-by-layer growth).

For a quantitative analysis, we consider the intensity at the first minimum (associated with the completion of the first monolayer) and the first maximum (associated with the completion of the second monolayer) and introduce the quantities δ_1 and δ_2 which describe the deviation from the ideal layer-by-layer growth: $\delta_{1,2}$ denote the percentage of molecules adsorbed in the “wrong” monolayer (see inset in fig. 3). At $t = \tau_{\text{ML}}$, $\theta_{\text{odd}} = 1 - \delta_1$, and $\theta_{\text{even}} = \delta_1$. If only two

monolayers contribute to the growth, δ_1 equals the coverage which is deposited in the second monolayer and which is missing in the first monolayer. At $t = 2\tau_{\text{ML}}$, *i.e.* after depositing the equivalent of 2 ML, the deviations from ideal layer-by-layer growth are analogously comprised in δ_2 , *i.e.* $\theta_{\text{odd}} = 1 + \delta_2$, and $\theta_{\text{even}} = 1 - \delta_2$. If the first monolayer is completely filled and only two monolayers contribute to the growth, δ_2 is the coverage deposited in the third layer and missing in the second layer. With this, the coverage difference (introduced in eq. (2)) can be expressed as

$$\Delta\theta(\tau_{\text{ML}}) = 1 - 2\delta_1 \quad \text{and} \quad \Delta\theta(2\tau_{\text{ML}}) = 2\delta_2. \quad (3)$$

Ideal layer-by-layer growth corresponds to $\delta_1 = \delta_2 = 0$. Figure 3 shows δ_1 and δ_2 as a function of T . For $T \gtrsim 358$ K, $\delta_1 \approx \delta_2 \approx 0$, as expected for ideal layer-by-layer growth. For decreasing temperatures, δ_1 and δ_2 increase continuously up to $\delta_1 \approx \delta_2 \approx 0.25$ with $\delta_2 \geq \delta_1$. The growth mode of the initial layers changes continuously with decreasing T and increasing deposition time from layer-by-layer to 3D growth.

The relation between these growth modes observed on a molecular scale during the deposition of the initial monolayers and the final, mesoscopic, morphology of the film (after deposition of about 15 ML [3]) can be rationalized with the following growth model. For $T \gtrsim 350$ K, we find large separate islands on two wetting monolayers. On a microscopic scale, the wetting layer grows in layer-by-layer mode, and then 3D nucleation occurs (SK growth). For $T \lesssim 350$ K, where the growth is more kinetically determined, relatively smooth films are observed after growth. On a microscopic scale, the films grow also in SK growth mode, but deviations of the layer-by-layer growth of the wetting layer are observed, and the density of the 3D nuclei on top of the wetting layer is much higher. Therefore, after the deposition of few monolayers the 3D nuclei grow together and form a closed but slightly rough film.

It has been shown that this growth mode change is accompanied by a change of the strain within the PTCDA film [3]. The influence of this change is within the experimental uncertainties of our measurements since the average electron density of one ML of PTCDA does not vary significantly with the strain. X-ray measurements of the specular rod indicate that the molecular stacking distance shows mainly the influence of the thermal expansion and not the strain. This is related to the van der Waals interaction between the molecules which changes only slightly with the strain-induced variations in the lateral ordering of the molecules. The thermal expansion has been taken into account in our measurements.

The question arises whether the observed growth mode follows from the specific molecular structure or can be mapped onto the concepts developed for inorganic MBE. In order to model the observed growth behavior and to identify the driving mechanisms of the 2D-3D transition including the temperature dependence of its dynamics, we performed kinetic Monte Carlo simulations at different growth temperatures in the range of 200 K to 300 K. The underlying solid-on-solid model is based on the bond-counting method and refined by including an interlayer transport barrier, E_{inter} , and an energy barrier E_{edge} for attachment/detachment from the step edges [16]. The effective energy barrier E_{inter} comprises various processes having an impact on the particle flow between neighboring layers including attractive substrate-adlayer interactions, strain, and the Ehrlich-Schwoebel barrier. It directly controls the 2D-3D transition: The important feature for the dynamics of the 2D-3D transition is the dependence of E_{inter} on the layer number n , namely $E_{\text{inter}}(n \leq 3) = 0$ and $E_{\text{inter}}(n > 3) > 0$. We note here that the absolute values used in the simulations are not relevant, but only the fact that $E_{\text{inter}}(n \leq 3) \ll E_{\text{inter}}(n > 3)$. As in the experiment, the only parameter varied is the substrate temperature.

At $t = 2\tau_{\text{ML}}$, our model exhibits a transition from layer-by-layer growth to islanding verified by the time-dependent autocorrelation function and the rms roughness, $\sigma(t)$, calculated from the simulations. This transition is smeared out for $T < 300$ K. After the 2D-3D transi-

tion, $\sigma(t)$ is steadily increasing with coverage. This increase is characteristic for SK growth and was found experimentally in a similar system (PTCDA/Au(111)) in post-growth studies [17].

From the simulation of the coverage of the individual layers, the time-dependent X-ray intensity at the anti-Bragg point can be calculated (see fig. 4). Remarkably, the assumption of a layer-dependent interlayer diffusion barrier, specifically the strong change of E_{inter} for $n > 3$ in our model, is sufficient to reproduce all essential features observed experimentally as a function of time and temperature, including the intensity oscillations for $t < 2\tau_{\text{ML}}$, their damping with decreasing temperature, the shift of the maximum, and the steady-state intensity for $t \gg 2\tau_{\text{ML}}$. The layer dependence of E_{inter} corresponds to the layer-dependent binding energy of the molecules. The first layer is strongly bound to the substrate, the second layer still feels some influence of the substrate, and the even lower binding energy of the subsequent layers cannot be distinguished anymore. Therefore, E_{inter} might be related to a competition between this binding energy and a Schwoebel barrier. In this model, at low layer numbers the strong influence of the binding energy favors layer-by-layer growth, while at higher layer numbers the influence of the Schwoebel barrier is larger than the influence of the binding energy, leading to 3D growth.

Given the relative simplicity of our model, it is not surprising that some differences between simulation and experiment are found. These are visible in the details of the damping and the intensity decrease after the maximum. The weak second minimum observed experimentally for very high temperatures is not reproduced in the simulations. This indicates that $E_{\text{inter}}(n = 4) < E_{\text{inter}}(n \rightarrow \infty)$. However, the kinetic Monte Carlo simulations show that the observed growth features can be directly mapped onto inorganic MBE. We note that, for comparison with an analytical model, we investigated a rate-equation approach similar to the one used by Vegt *et al.* [18] with the effective interlayer diffusion constant k_n . Our analysis shows that k_n has to change dramatically between $n = 2$ and $n = 3$, similar to $E_{\text{inter}}(n)$ in our kMC simulations in order to reproduce the experimental data.

In conclusion, a detailed study of organic-inorganic heteroepitaxial growth has been reported for PTCDA on Ag(111) as an archetypal system for organic MBE. The system PTCDA/Ag(111) exhibits Stranski-Krastanov growth. The temperature dependence of the transition from layer-by-layer growth to island growth has been observed in real time and analyzed quantitatively. The 2D-3D transition is smeared out for low growth temperatures. This behavior has been reproduced by kinetic Monte Carlo simulations and a rate-equation approach. Both approaches show the importance of the layer-dependence of the interlayer transport for the 2D-3D transition.

It is instructive to compare our results with a similar X-ray study of the growth of Xe on Ag(111) [14], which exhibits a continuous decay of the growth oscillations, in contrast to the rather distinct change observed in our case. Apparently these differences reflect the different nature of the underlying interactions to the substrate. Both materials form van der Waals crystals. Xe is weakly physisorbed at the Ag interface, while PTCDA is more strongly bound [19]. Due to the strong binding, the first layer of PTCDA is strained, and the SK growth might be a way to relax this strain.

Another well-studied van der Waals system are the n-alkanes. Similar to PTCDA, these molecules show SK growth if they are deposited on Ag(111) [2]. A change in the molecular tilt with respect to the substrate surface has been assumed to be the reason for the observed SK growth. However, this argument does not hold for the dewetting of PTCDA since all molecular layers of PTCDA grow with the molecular plane parallel to the substrate surface [19].

Our results have several implications for the understanding and the modelling of the growth of organic molecules. The observed interplay of the kinetics and the energetics provides a way to understand the growth and the evolution of the morphology of organic films on a microscopic

level and thus shows how it may be controlled either by external parameters or by changing specific functional groups of the molecules to tailor the interactions and the associated diffusion barriers. The latter is a unique feature of organics, which may be exploited in future studies.

* * *

We are grateful to N. KARL for providing the purified material. We wish to thank A. C. DÜRR and K. A. RITLEY for their help with the experiments, and A. VIDECOQ for the introduction to the program used for the kinetic Monte Carlo simulations. We thank the HASYLAB staff for technical support. Partial support from the DFG (Schwerpunktprogramm "Organische Feldeffekt-Transistoren") is gratefully acknowledged.

REFERENCES

- [1] MEYER ZU HERINGS DORF F.-J., REUTER M. C. and TROMP R. M., *Nature*, **412** (2001) 517.
- [2] WU Z., EHRLICH S. N., MATTHIES B., HERWIG K. W., DAI P., VOLKMAN U. G., HANSEN F. Y. and TAUB H., *Chem. Phys. Lett.*, **348** (2001) 168.
- [3] KRAUSE B., DÜRR A. C., RITLEY K., SCHREIBER F., DOSCH H. and SMILGIES D., *Phys. Rev. B*, **66** (2002) 235404.
- [4] CHKODA L., SCHNEIDER M., SHKLOVER V., KILIAN L., SOKOLOWSKI M., HESKE C. and UMBACH E., *Chem. Phys. Lett.*, **371** (2003) 548.
- [5] BAUER E. and VAN DER MERWE J. H., *Phys. Rev. B*, **33** (1986) 3657.
- [6] MÜLLER P. and KERN R., *Appl. Surf. Sci.*, **102** (1996) 6.
- [7] WOLL A. R., HEADRICK R. L., KYCIA S. and BROCK J. D., *Phys. Rev. Lett.*, **83** (1999) 4349.
- [8] NICKLIN C. L., NORRIS C., STEADMAN P., TAYLOR J. S. G. and HOWES P. B., *Physica B*, **221** (1996) 86.
- [9] FENTER P., EISENBERGER P., BURROWS P., FORREST S. R. and LIANG K. S., *Physica B*, **221** (1996) 145.
- [10] GLÖCKLER K., SEIDEL C., SOUKOPP A., SOKOLOWSKI M., UMBACH E., BÖHRINGER M., BERNDT R. and SCHNEIDER W.-D., *Surf. Sci.*, **405** (1998) 1.
- [11] KRAUSE B., DÜRR A. C., RITLEY K. A., SCHREIBER F., DOSCH H. and SMILGIES D., *Appl. Surf. Sci.*, **175-176** (2001) 332.
- [12] KRAUSE B. *et al.*, in preparation.
- [13] Vlieg E., DENIER VAN DER GON A. W., VAN DER VEEN J. F., MACDONALD J. E. and NORRIS C., *Phys. Rev. Lett.*, **61** (1988) 2241.
- [14] DAI P., WU Z., ANGOT T., WANG S.-K., TAUB H. and EHRLICH S. N., *Phys. Rev. B*, **59** (1999) 15464.
- [15] RITLEY K., KRAUSE B., SCHREIBER F. and DOSCH H., *Rev. Sci. Instrum.*, **72** (2001) 1453.
- [16] PIMPINELLI A. and VILLAIN J., *Physics of Crystal Growth* (Cambridge University Press, Cambridge) 1999.
- [17] FENTER P., SCHREIBER F., ZHOU L., EISENBERGER P. and FORREST S. R., *Phys. Rev. B*, **56** (1997) 3046.
- [18] VAN DER VEGT H. A., HUISMAN W. J., HOWES P. B., TURNER T. S. and Vlieg E., *Surf. Sci.*, **365** (1996) 205.
- [19] TABORSKI J., VÄTERLEIN P., DIETZ H., ZIMMERMANN U. and UMBACH E., *J. Electron Spectrosc. Relat. Phenom.*, **75** (1995) 129.